Double folding optical parameters for 240 MeV ^{6}Li beam -revisited

Y. Xu, J. Button, Y. -W. Lui, and D. H. Youngblood

I. Nuclear density distribution

We collect 4 kinds of 6Li nuclear density distributions for constructing the nuclear double folding potentials between ^{6}Li projectile and seven target nuclei (^{24}Mg, ^{28}Si, ^{40}Ca, ^{48}Ca, ^{58}Ni, ^{90}Zr, and ^{116}Sn). These nuclear density distributions are the theoretical results from *ab initio* [1], COSMA [2], and HFB [3], as well as the experimental results by electron scattering [4]. Fig. 1 shows the comparison of these 4 kinds of nuclear density distributions for ^{6}Li. We finally choose the adopted experimental results [4] as the ^{6}Li projectile density distributions for the construction of nuclear double folding potential.

On the other hand, we employ the calculated results by HFB theory [3] as the density distributions of the 7 target nuclei for the construction of nuclear double folding potential.

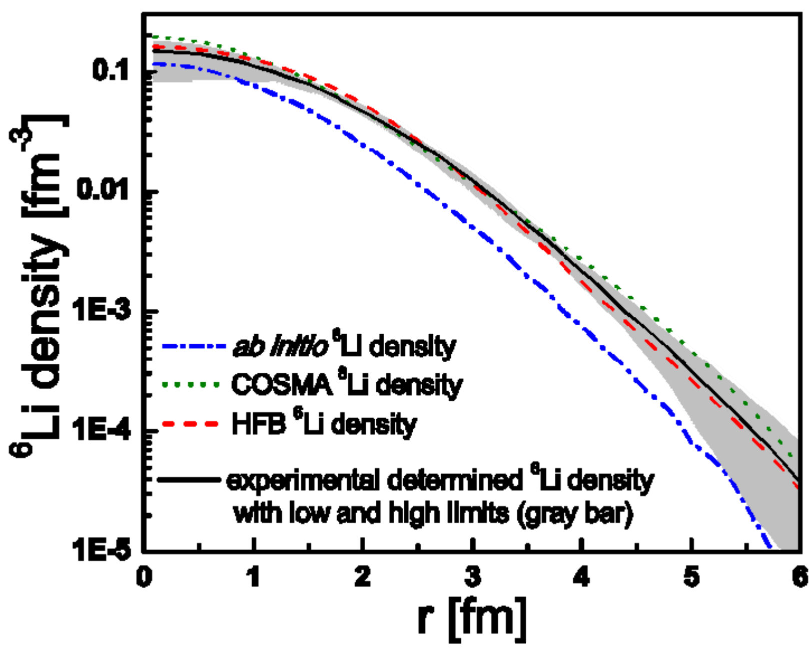

FIG. 1. Comparison of the different nuclear density distributions for ^{6}Li.

II. Nuclear DDM3Y double folding potential

By folding the nuclear densities (both projectile and target) and nucleon-nucleon interaction, we obtained the DDM3Y double folding potentials between ^{6}Li and these 7 target nuclei. The detail folding method could be found in Refs. [5, 6]. Fig. 2 shows such DDM3Y double folding potential between ^{6}Li and ^{116}Sn as the example, where the 4 kinds of ^{6}Li density distributions are all presented.

We finally choose the DDM3Y double folding potential, deduced by ^{6}Li experimental density distribution, as the real part of nuclear potential in the further fitting of elastic data.

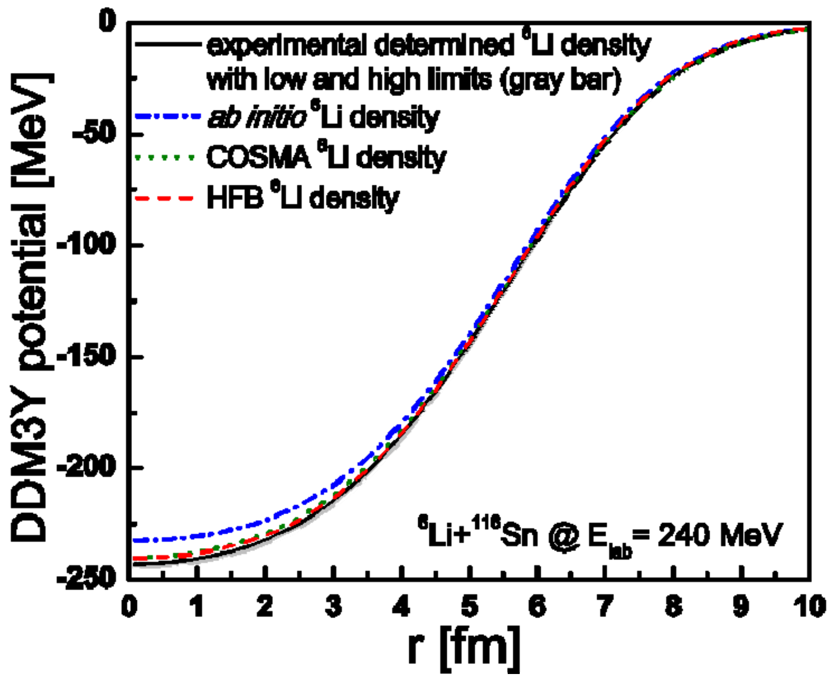

FIG. 2. DDM3Y double folding potential between 6Li and 116Sn. The 4 kinds of 6Li density distributions are all presented.

III. Elastic scattering fitting

By using the ECIS06 code, we fit the experimental data (angular distributions) of ^{6}Li elastic scattering on these 7 target nuclei at $E_{c.m.}$=240MeV. During the fitting, the DDM3Y double folding potential (as described in Part II) is adopted as the real part, while the Wood-Saxon potential is adopted as the imaginary part. Such choice is similar to those in Refs [5, 6]. To obtain the best fitting, a normalized factor and a scaling factor are introduced for the DDM3Y double folding potential. For the elastic scattering between 6Li and these 7 target nuclei, Fig. 3 shows the fitting results and Table I lists the corresponding potential parameters and χ^2 for Fig. 1.

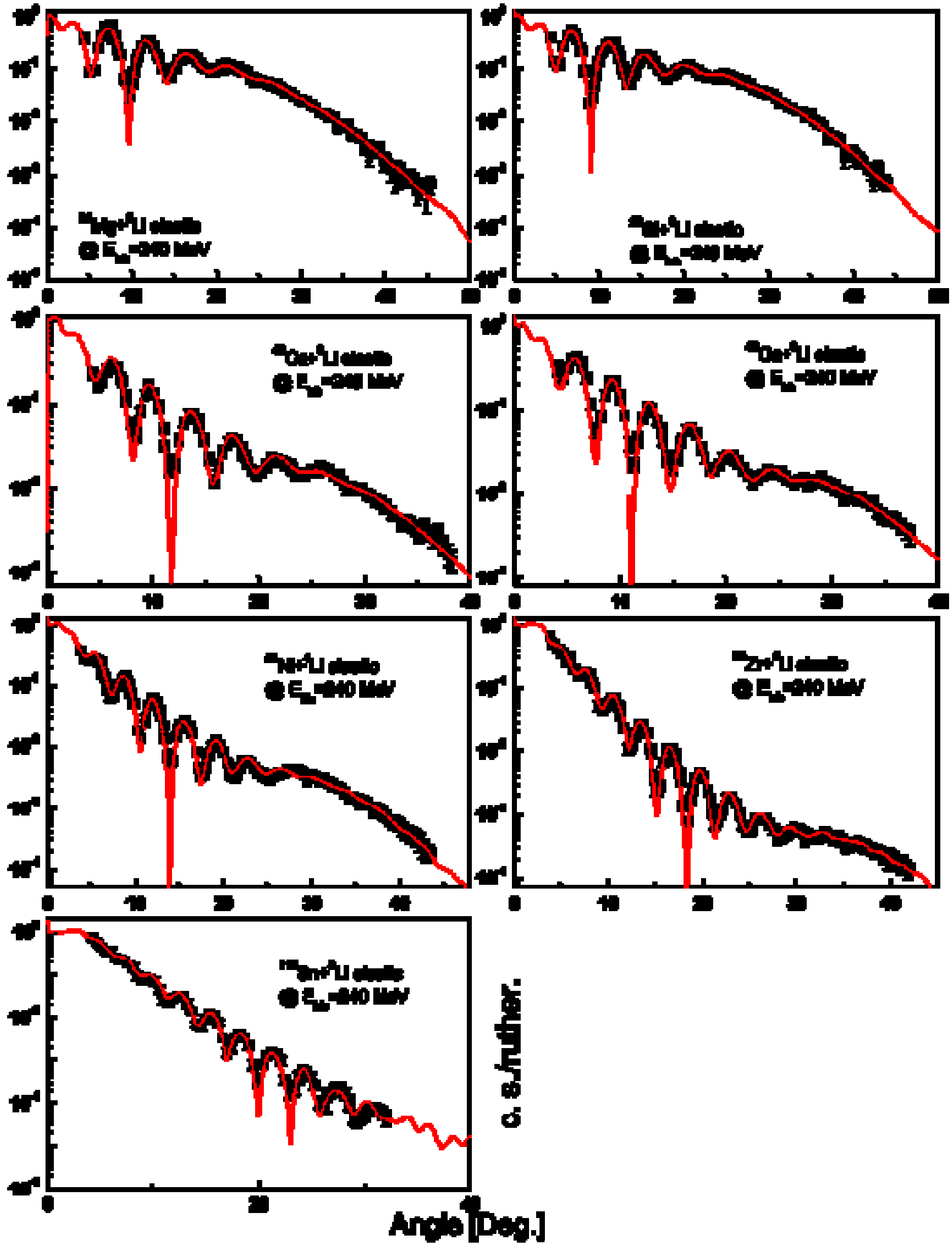

FIG. 3. The fitting results of ^{6}Li elastic scattering on ^{24}Mg, ^{28}Si, ^{40}Ca, ^{48}Ca, ^{58}Ni, ^{90}Zr, and ^{116}Sn at $E_{c.m.}$=240MeV.

Table I. The parameters for DDM3Y potential and Wood-Saxon potential and χ^2 for Fig. 1.

Z	N	A	Nuclei	Normalized	Scaling factors	V	r	a	X^2	previous X^2
				DDM3Y real part		Wood-Saxon imaginary part				for comparison
12	12	24	24Mg	0.852	1.0587	50.28739	4.00815	1.07187	1.101	1.039
14	14	28	28Si	0.8598	1.0512	42.69501	4.4028	1.04332	1.343	1.461
20	20	40	40Ca	0.8672	1.0717	44.45008	4.86415	1.09883	1.637	1.7
20	28	48	48Ca	0.8823	1.0653	32.99495	5.74968	0.90051	1.134	1.2
28	30	58	58Ni	0.8496	1.0608	39.60765	5.67734	1.08959	1.222	0.9
40	50	90	90Zr	0.8566	1.0561	35.07076	6.87215	0.98615	0.905	1.1
50	66	116	116Sr	0.8502	1.0658	59.11377	6.68749	1.04347	1.396	1.19

Furthermore, we also fit the obtained 7 sets of normalized factors and the scaling factors against the nuclear mass number, which are shown in Fig. 4. It is expected to predict these (normalized and scaling factors) parameters for ^{6}Li elastic scattering on other target nuclei.

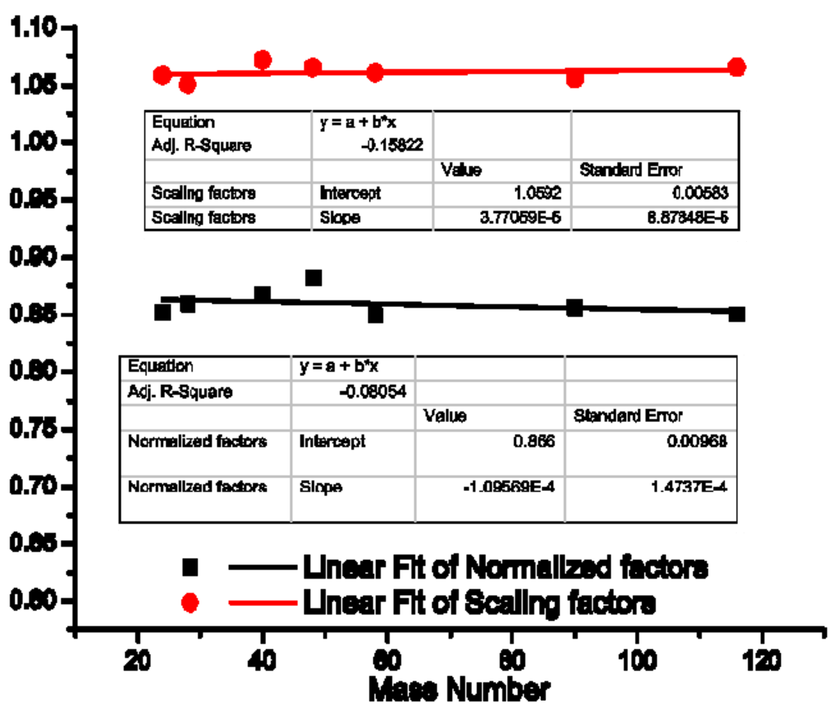

FIG. 4. The fitting results of obtained normalized factors and the scaling factors against the nuclear mass number for the 7 sets of elastic scattering.

IV. Inelastic scattering calculation

According to the nuclear potential (DDM3Y real part and Wood-Saxon imaginary part) obtained by elastic scattering fitting, we calculate the angular distributions of the differential cross sections for 6Li inelastic scattering to the low-lying excited states of these 7 target nuclei. Here, the results for ^{24}Mg (2^+ state at E*=1.369MeV), ^{28}Si (2^+ state at E*=1.779MeV and 3^- state at E*=6.888MeV) and ^{116}Sn (2^+ state at E*=1.29MeV and 3^- state at E*=2.27MeV) are shown in Fig. 5.

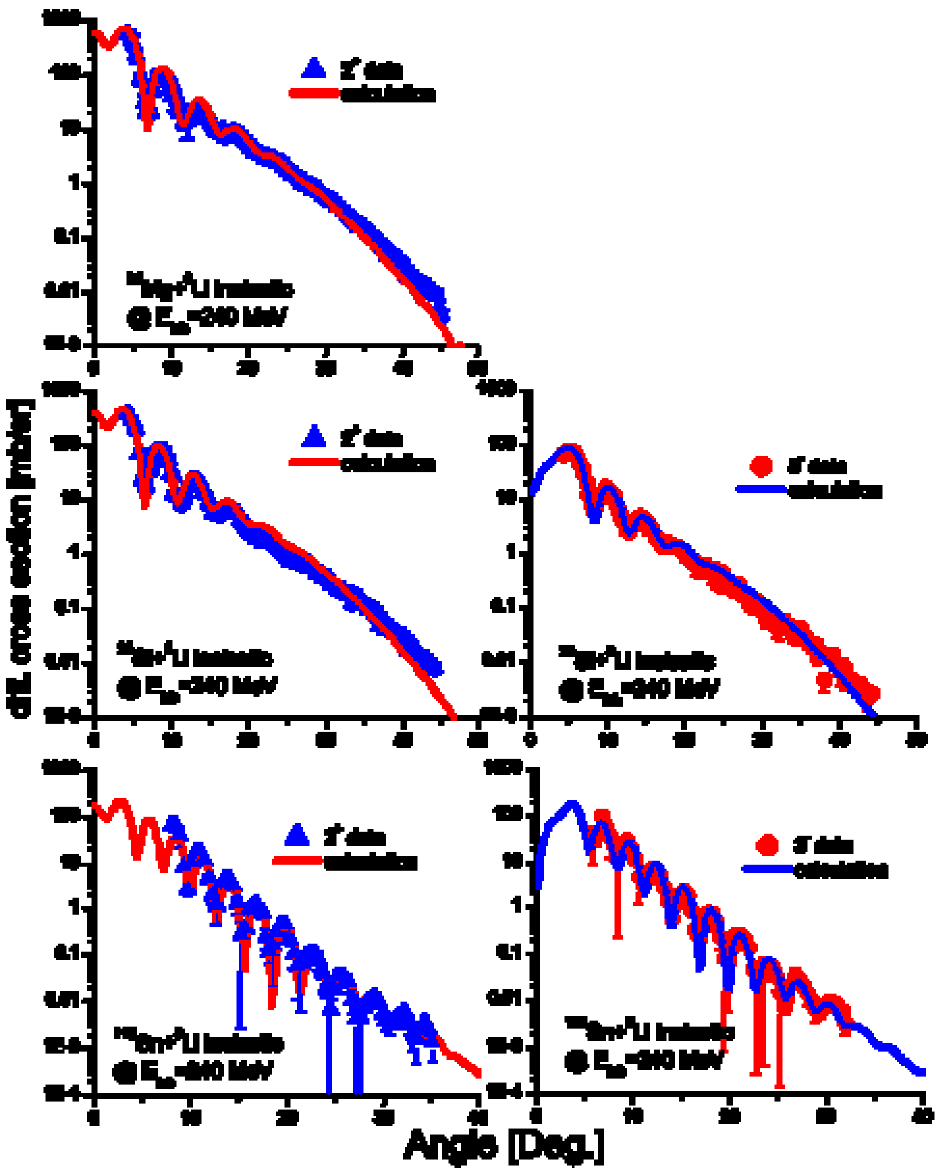

FIG. 5. The angular distributions of ^{6}Li inelastic scattering to the low-lying excited states of ^{24}Mg, ^{28}Si and ^{116}Sn

During the calculations, the transfer potentials to low-lying excited states [5, 7] are taken into account, thus the reduced transition possibilities, namely the B(E2) and B(E3) values, are deduced. The procedure of extracting the B(EL) value is described in Refs. [5,7,8]. Here, we obtained that B(E2) =0.0451 for 2^+ state of ^{24}Mg (E*=1.369MeV), B(E2) =0.0317 for 2^+ state of ^{28}Si (E*=1.779MeV), B(E3)=0.00305 for 3^- state of ^{28}Si (E*=6.888MeV), B(E2) =2.30 for 2^+ state of ^{116}Sn (E*=1.29MeV), and B(E3)=1.28 for 3^- state of ^{116}Sn (E*=2.27MeV). The results for other 4 nuclei are still on studying.

[1] C. Cockrell *et al.*, Phys. Rev. C **86**, 034325 (2012).

[2] A.A. Korsheninnikov *et al.*, Nucl. Phys. **A617**, 45 (1997).

[3] Y. Xu *et al.*, Astron. Astrophys. **549**, A106 (2013), and S. Goriely, private communication

[4] A.V. Dobrovolsky *et al.*, Nucl. Phys. **A766**, 1 (2006).

[5] X. Chen *et al.*, Phys. Rev. C **76**, 054606 (2007).

[6] X. Chen *et al.*, Phys. Rev. C **80**, 014312 (2009).

[7] X. Chen et al., Phys. Rev. C **79**, 024320 (2009).

[8] H.L. Clark *et al.*, Phys. Rev. C **57**, 2887 (1998).